Cool Stars, Stellar Systems and the Sun
ASP Conference Series, Vol. 154, 1998
eds. R. A. Donahue and J. A. Bookbinder

The Contribution of Flares to Transition Region Heating in Active G and K Dwarfs

S.H. Saar and J.A. Bookbinder

Smithsonian Astrophysical Observatory, Cambridge, MA 02138

Abstract:

We present the preliminary results of an analysis of *HST* GHRS rapid readout spectra covering the region 1380Å - 1670Å for two active dwarfs of approximately Pleiades age: HD 129333 (G0V, $P_{\rm rot} \approx 2.8$ days) and LQ Hya (K2V, $P_{\rm rot} \approx 1.6$ days). Both were observed for $\geq$4 orbits at 1 second time resolution (total exposure time > 13,000 s each). The time series of the transition region (TR) fluxes (the sum of C IV + Si IV) shows many low-level flares in both stars, making the quiescent level somewhat difficult to identify. We assume that TR heating in the stars is a combination of a steady background (due to e.g., MHD wave heating) plus superimposed flares. The distribution of TR photons per unit time, $N(n_{\rm TR})$, should thus have a component at the low counts which can be fit by a Poisson function. The best-fit Poisson to the low count end of $N(n_{\rm TR})$ then defines the the average background TR heating rate (from the Poisson mean), and an upper limit to the total steady heating unaffected by flares (from the Poisson amplitude). Our analysis suggests that at least 8% of TR flux of HD 129333 and 11% of TR flux of LQ Hya arose from flares during our observations. We also discuss the flare rates as a function of energy. This represents the first detailed information on flare heating rates for active G and K dwarfs.

1. Introduction

Flares on late K and M stars are much studied, but little is known about flare energies or rates for G and early K stars. This is largely due to a contrast effect; at optical wavelengths (where most of the work has been done) the signatures of flares difficult to distinguish against the bright continuua of G and K stars, except in rare cases (e.g., Montes et al. 1998). In the UV and X-rays, where flares are more obvious, instruments have generally been sensitive enough to see only the top of the flare distribution (e.g., π^1 UMa; Landini et al. 1986).

Flares are proposed to be an important contributor to coronal heating in active G and K stars (e.g., Güdel et al. 1997a), in particular of the higher temperature plasma (Schrijver et al. 1995; Güdel 1997). To explore the significance of flares to atmospheric heating in G and K stars, we have studied four active stars with *HST* at high time resolution. We report here on initial results for two of the stars.

CD–1560

2. Observations and Reduction

Two very active targets were selected: HD 129333 (EK Dra), a G0 dwarf in the Pleiades moving group (age ~ 0.07 Gyr) and a rotational period of $P_{\rm rot} = 2.75$ days (e.g., Güdel et al. 1997b); and LQ Hya (HD 82558) a K2 dwarf of similar age and $P_{\rm rot} = 1.6$ days (e.g., Strassmeier et al. 1993). Both were observed with GHRS G140L in rapid readout mode (1 s resolution); HD 129333 for 4 orbits (19600 s exposure time on UT 16 Feb 1996; the star is in the continuous viewing zone) and LQ Hya for 5 orbits (13220 s exposure time over a 430 min interval on UT 7 Nov 1995). This amounts to a rotational phase interval of $\Delta\phi = 0.08$ for HD 129333 and $\Delta\phi = 0.18$ for LQ Hya. While this represents a non-negligible fraction of $P_{\rm rot}$, we detect little evidence for significant variation in the quiescent flux on these timescales.

The data were processed and analyzed with standard *HST* software and special purpose software written in IDL. After examining the time averaged spectra for each orbit, we identified integration windows for lines of interest and summed the counts in each window for each 1 second timestep. Here, we focus on transition region (TR) emission - specifically, the time series of the total Si IV ($T_{\rm form} \sim 80,000$ K) and C IV ($T_{\rm form} \sim 10^5$ K) counts, $n_{\rm TR}$, for three time binnings (5, 10 and 30 s; Fig. 1).

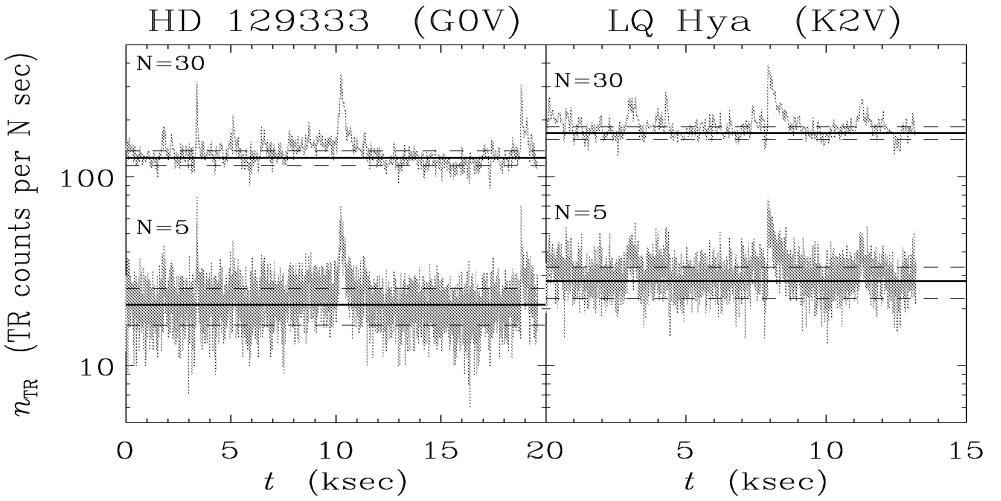

Figure 1. Counts per N seconds (N=5 and 30) in TR lines (C IV + Si IV), $n_{\rm TR}$ (gray), versus time for HD 129333 (left) and LQ Hya (right). The mean counts μ of the estimated quiescent component (derived from a Poisson fit; see text and later figures) and $\pm\sqrt{\mu}$ levels are indicated (solid and dashed horizontal lines, respectively).

3. Analysis and Results

We made the simplifying assumption that there are only two processes responsible for the TR line formation:

1. a quiescent process which is constant (or only slowly varying) in time (e.g., steady MHD wave heating), and
2. a stochastic, impulsive, highly time variable process (i.e., flares and microflares)

With this assumption, the quiescent component can be modeled as a Poisson distribution of photon counts about some constant mean, μ. The flare component is then any excess over this. In the limit that there are *no* flares contributing to $n_{\rm TR}$ at low count levels, we can fit the lower energy bins of the photon count distribution $N(n_{\rm TR})$ with a Poisson function. By varying the Poisson mean and amplitude to find the best fit, we derive an *upper limit* on the portion of quiescent component completely unaffected by flares (Fig. 2, dashed). Subtraction of the

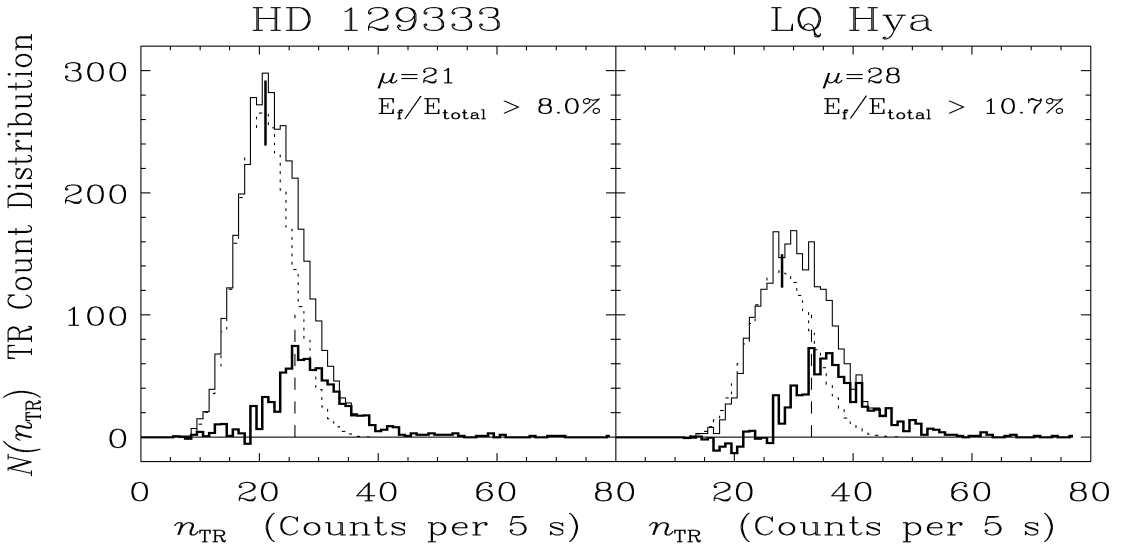

Figure 2. Distribution of TR counts $N(n_{\rm TR})$ versus $n_{\rm TR}$ for HD 129333 (left) and LQ Hya (right) with 5 s binning (solid), plus a Poisson fit to the low $n_{\rm TR}$ part of the distribution (dotted), and the residual (thick solid). The Poisson mean μ (heavy vertical line) and $\mu + \sqrt{\mu}$ (dashed vertical line) used to define the minimum flare level, are also shown. The Poisson fit represents the maximum quiescent component undisturbed by flares. If there were *no* flares at all, the area of the Poisson would $= \Sigma N(n_{\rm TR})$. The difference between the observed $N(n_{\rm TR})$ and the flux implied by this scaled "quiescent" Poisson is then a measure of the *minimum* total flare flux E_f. For HD 129333, $E_f/E_{\rm total}$ >8.0%, for LQ Hya, $E_f/E_{\rm total}$ >10.7%.

Poisson distribution from the total generates an estimate of the minimum distribution of photons arriving in time intervals with flares (Fig. 2, thick solid). The

same "quiescent" distribution, scaled in amplitude so that its integral matches the total number of time samples, yields an estimate of the what the star would look like with *no* flares, which is effectively an *upper limit to the total quiescent component*. The difference between the observed total TR flux, and the TR flux implied by this maximum "all quiet" distribution, produces a *lower limit* to the flare contribution to the total TR flux. For HD 129333, the difference between these two distributions implies that the fraction of TR energy in flares is at least $E_f/E_{\rm total}$ >8.0%; for LQ Hya, the value is $E_f/E_{\rm total}$ >10.7%.

The "quiescent Poisson fitting" technique we employ is actually somewhat involved, since it is not immediately clear how many bins at the low end of $N(n_{\rm TR})$ *should* be fit for a Poisson of given μ. To determine an optimal fit, we searched for the highest signal-to-noise of the Poisson fit. In practice, this meant we found the optimum Poisson amplitude to fit the lower end $N(n_{\rm TR})$ for a given μ and fit interval, with the fit diagnostic being a minimum in the ratio of the weighted fit RMS to the total number of time intervals fit. An example of a contour map of fit RMS/total intervals shows the optimum solution for LQ Hya at 5 s time binning (Fig. 3) - the resulting fit is in Fig. 2 (right panel).

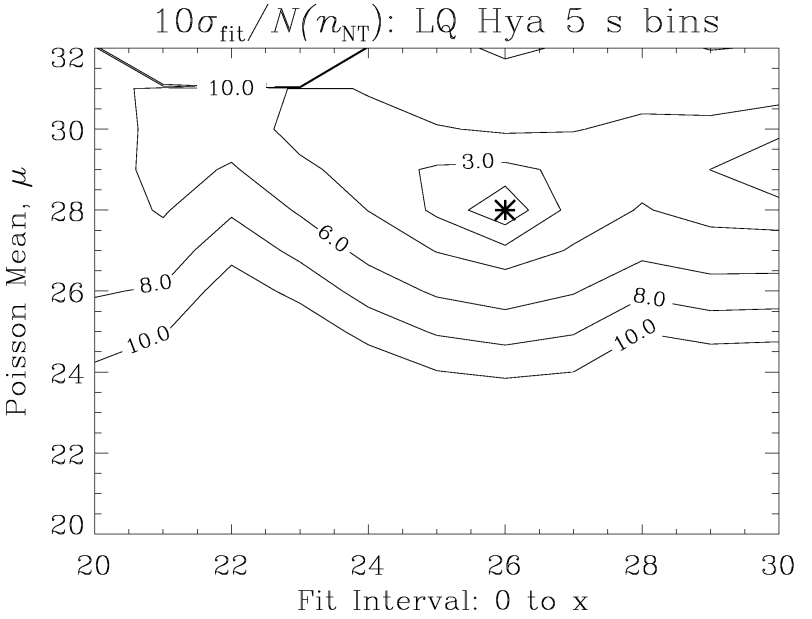

Figure 3. Contour plots of $\sigma_{\rm fit}/N(n_{\rm TR})$, the S/N of the Poisson fit, as a function of the Poisson mean μ, and the interval over which $N(n_{\rm TR})$ is fit. The minimum ($*$) implies the best-fit $\mu = 28$ (indicated by the horizontal solid line in Fig. 1-right, and the vertical solid line in Fig. 2-right). This μ, combined with the amplitude generated by the fit, defines the "quiescent Poisson" shown in Fig. 2-right (dotted).

While the above analysis yields an estimate of the minimum flare (and microflare) contribution to the total flux, since it deals with distributions, it does not say anything about individual flares themselves. To study these, for this preliminary analysis we use the optimum μ values determined from the Poisson fits, and define flares as being all time intervals with TR counts above $\mu+\sqrt{\mu}$ (Fig. 1; upper dashed lines). Though simplistic, and inevitably leading to

some contamination (at low flare energies E_f) by the upper end of the quiescent distribution, it is at least a statistically robust definition.

Using our simple flare definition, we computed flare durations, Δt (time above $\mu + \sqrt{\mu}$) and total energies E_f (in counts) for all flare events. Study of flare energy distributions, $N(E_f)$ (Fig. 4) allow us to compare easily with previous results. If we discount $N(E_f)$ at low E_f (due to contamination by the

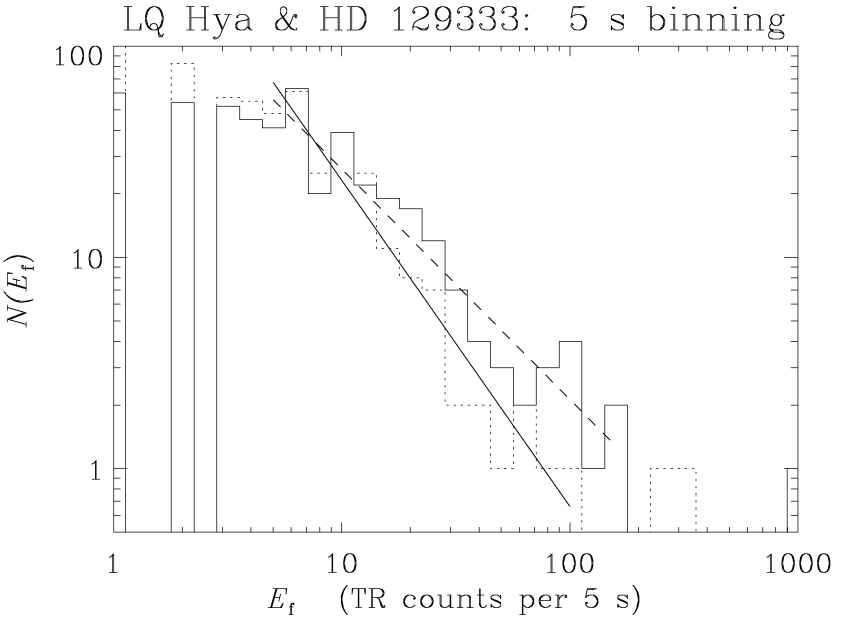

Figure 4. Distribution of TR flare energies $N(E_f)$ versus E_f (in counts) for LQ Hya (solid histogram) and HD 129333 (dotted histogram) with 5 s binning; E_f are determined by integrating counts above $\mu + \sqrt{\mu}$ for a given event. Power law fits (for the interval indicated by the line length) are also shown: $N(E_f) \propto E_f^{-1.1}$ for LQ Hya (dashed line) and $N(E_f) \propto E_f^{-1.5}$ for HD 129333 (solid line).

quiescent component and noise) and at very high E_f (due to poor statistics) and just fit the middle range of the distributions, we find

$N(E_f) \propto E_f^{-1.5\pm0.1}$ (HD 129333; 5, 10, & 30s binning intervals)

and

$N(E_f) \propto E_f^{-1.0\pm0.1}$ (LQ Hya; 5, 10, & 30s binning intervals)

In general the fits to the 30 s binning $N(E_f)$ were rather poor, due to poor statistics on numbers of flares.

If we study E_f as a function of flare duration Δt (weighting by E_f to reduce the effects of small noise spikes) we find (Fig. 5):

$E_f \propto \Delta t^{1.4\pm0.1}$ (HD 129333 & LQ Hya; 5, 10, 30s bins)

4. Discussion

It is perhaps not surprising that $\geq 10\%$ of the TR flux from active G and K stars arises from flares. As noted in the introduction, flares are believed responsible

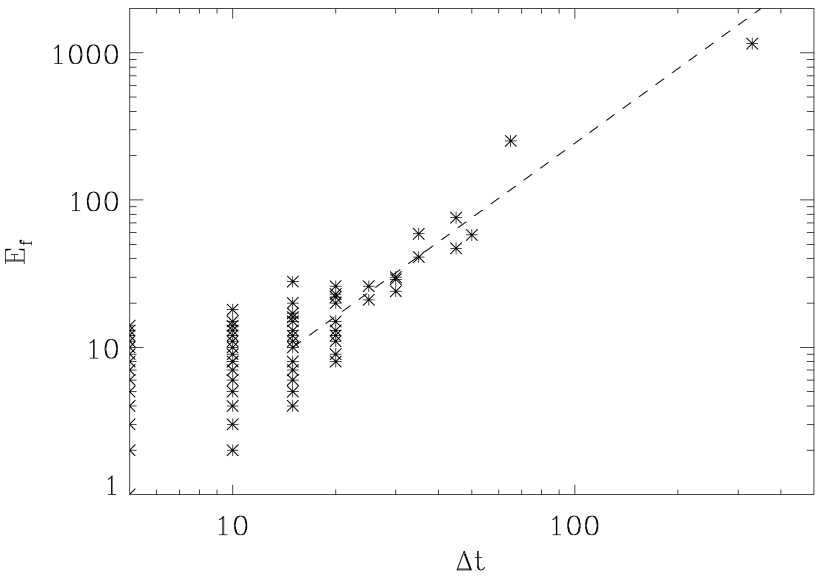

Figure 5. TR flare energy E_f (defined as in Fig. 4) versus duration Δt for HD 129333 with 30 s binning; a fit (weighted by E_f) yields $E_f \propto \Delta t^{1.4}$ (dashed).

for the ubiquitous hot component of the coronal plasma in active stars which provides a substantial fraction of the total coronal emission measure. Our results lend direct support for this hypothesis.

Shimizu (1995) found $N(E_f) \propto E_f^{-1.5}$ to $E_f^{-1.6}$ for transient events in the *Yohkoh* solar soft X-ray data. Similarly, Crosby et al. (1993) derived $N(E_f) \propto E_f^{-1.5}$ for solar hard X-rays from *SMM*. A recent model of a turbulently driven 2-D loops predict a similar dependence (Dmitruk & Gomez 1997). These are remarkably similar to our result for HD 129333 (Fig. 4), which has been used as a proxy for the young Sun (Güdel et al. 1997a). HD 129333 thus has a flare energy distribution similar to the Sun, but uniformly scaled in number up at all E_f. The results for LQ Hya imply a larger contribution from higher E_f flares (Fig. 4) than is seen on the Sun or HD 129333. The correlation between total E_f and flare duration is shallower than predicted by loop ($E_f \propto \Delta t^2$; Dmitruk & Gomez 1997) or avalanche ($E_f \propto \Delta t^{1.8}$; Lu et al. 1993) flare models. Observationally, the data shown in Lu et al. (1993; their Fig. 7) suggest $E_f \propto \Delta t^{1.4}$ (Lee et al. 1993 derive $E_{f,max} \propto \Delta t^{1.7}$ from the same dataset, where $E_{f,max}$ is the peak flare rate). Thus our result, $E_f \propto \Delta t^{1.4}$ (Fig. 5) is consistent with solar observations and slightly shallower than theoretical models. Interestingly, here the same law holds for both the G and the K star.

Acknowledgments. This work was based on observations obtained with the NASA *Hubble Space Telescope*, which is operated by AURA under NASA contract NAS5–26555. SS and JB were supported by NASA *HST* grant GO–05871.01–94A. We thank M. Güdel for helpful discussions.

References

Crosby, N.B., Aschwanden, M.J., & Dennis, B.R. 1993, Solar Phys., 143, 275

Dmitruk, P., & Gomez, D.O. 1997, ApJ, 484, L83

Güdel, M. 1997, ApJ, 480, L121

Güdel, M., Guinan, E.F., & Skinner, S.L. 1997a, ApJ, 483, 947

Güdel, M., Guinan, E.F., Mewe, R., Kaastra, J.S., & Skinner, S.L. 1997b, ApJ, 479, 416

Landini, M., Monsignori Fossi, B.C., Pallavicini, R., & Piro, L. 1986, A&A, 157, 217

Lee, T.T., Petrosian, V., & McTiernan, J.M. 1993, ApJ, 412, 401

Lu, E.T., Hamilton, R.J., McTiernan, J.M., & Bromund, K.R. 1993, ApJ, 412, 841

Montes, D., Saar, S.H., Collier Cameron, A., Unruh, Y.C. 1998, in ASP Conf. Ser. 154, The Tenth Cambridge Workshop on Cool Stars, Stellar Systems and the Sun, eds. R.A. Donahue & J.A. Bookbinder (San Francisco: ASP), 1508

Schrijver, C.J., van den Oord, G.H.J., Mewe, R., & Kaastra, J.S. 1995, A&A, 302, 438

Shimizu, T. 1995, PASJ, 47, 251

Strassmeier, K.G., Rice, J.B., Wehlau, W.H., Hill, G.M., Matthews, J.M. 1993, A&A, 241, 167

Stellar Winds, Mass Loss, Evolved Stars

CD–1567